

9-1-2006

# Crop yield prediction using multipolarization radar and multitemporal visible / infrared imagery

Graeme G. Wilkinson

*Glyndwr University, g.wilkinson@glyndwr.ac.uk*

I. C. Davies

Follow this and additional works at: <http://epubs.glyndwr.ac.uk/cair>

 Part of the [Databases and Information Systems Commons](#), and the [Numerical Analysis and Scientific Computing Commons](#)

## Recommended Citation

Davis, I.C. & Wilkinson, G.G. (2006) 'Crop yield prediction using multipolarization radar and multitemporal visible / infrared imagery'. In Remote Sensing for Agriculture, Ecosystems, and Hydrology VIII, SPIE Conference 6359. Stockholm, Sweden

This Other is brought to you for free and open access by the Computer Science at Glyndŵr University Research Online. It has been accepted for inclusion in Computing by an authorized administrator of Glyndŵr University Research Online. For more information, please contact [d.jepson@glyndwr.ac.uk](mailto:d.jepson@glyndwr.ac.uk).

---

# Crop yield prediction using multipolarization radar and multitemporal visible / infrared imagery

## **Abstract**

This paper describes research undertaken on the improvement of within-field late season yield forecasting for crops such as wheat using multi-temporal visible/infrared satellite imagery and multi-polarization radar satellite imagery. Experiments have been carried out using ASAR imagery from Envisat combined with nine bands of ASTER imagery from the NASA Terra satellite. An experimental test site in an agricultural area in the county of Lincolnshire, UK, has been used. The satellite imagery has been integrated using artificial neural networks which have been trained as predictors of the spatial distributions of yield per unit area in a variety of fields. Ground truth data in the form of yield maps from GPS-enabled combine harvesters have been used to train the neural networks and to evaluate accuracy. The results show that the combinations of ASTER and ASAR imagery can provide enhanced yield predictions with overall correlations of up to 0.77 between predicted and actual yield patterns. The results also show that the use of dual polarization radar data alone is not sufficient to give reasonable yield predictions even in a multi-temporal mode. It has also been shown that varying the architectures of the neural networks with ensembles can improve the overall results.

## **Keywords**

Agriculture, remote sensing, yield prediction, radar imagery, multi-temporal data, multi-polarization.

## **Disciplines**

Computer Sciences | Databases and Information Systems | Numerical Analysis and Scientific Computing

## **Comments**

©Copyright 2009 SPIE Society of Photo - Optical Instrumentation Engineers. One print or electronic copy may be made for personal use only. Systematic electronic or print reproduction and distribution, duplication of any material in this paper for a fee or for commercial purposes, or modification of the content of the paper are prohibited. This paper was given at the SPIE Conference 6359 Remote Sensing for Agriculture, Ecosystems, and Hydrology VIII conference in Stockholm in september 2006. The SPIE conference paper is available at <http://spiedl.aip.org>

# Crop yield prediction using multipolarization radar and multitemporal visible / infrared imagery

Ian C. Davis, Graeme G. Wilkinson  
Centre for Visual Surveillance and Machine Perception Research,  
Faculty of Technology, University of Lincoln, Brayford Pool, Lincoln, LN6 7TS, UK.

## ABSTRACT

This paper describes research undertaken on the improvement of within-field late season yield forecasting for crops such as wheat using multi-temporal visible/infrared satellite imagery and multi-polarization radar satellite imagery. Experiments have been carried out using ASAR imagery from Envisat combined with nine bands of ASTER imagery from the NASA Terra satellite. An experimental test site in an agricultural area in the county of Lincolnshire, UK, has been used. The satellite imagery has been integrated using artificial neural networks which have been trained as predictors of the spatial distributions of yield per unit area in a variety of fields. Ground truth data in the form of yield maps from GPS-enabled combine harvesters have been used to train the neural networks and to evaluate accuracy. The results show that the combinations of ASTER and ASAR imagery can provide enhanced yield predictions with overall correlations of up to 0.77 between predicted and actual yield patterns. The results also show that the use of dual polarization radar data alone is not sufficient to give reasonable yield predictions even in a multi-temporal mode. It has also been shown that varying the architectures of the neural networks with ensembles can improve the overall results.

**Keywords:** Agriculture, remote sensing, yield prediction, radar imagery, multi-temporal data, multi-polarization.

## 1. INTRODUCTION

Satellite remote sensing continues to offer much promise for agriculture, particularly in the context of so-called smart farming<sup>1</sup>. Although there are many potential applications of remote sensing in agriculture, one which is paramount is the prediction of crop yield<sup>2</sup>. Yield prediction has various purposes depending on the stage in the phenological cycle, the spatial resolution and the geographic coverage at which it takes place. Low resolution yield prediction at continental scale can be of benefit to major food import and export companies and to international governmental agencies who are concerned with global markets and prices and the potential impact of shortages and surpluses. Remote sensing based on low resolution meteorological satellites has been particularly useful in this regard<sup>3</sup>. High resolution yield prediction can benefit individual farms and food production companies. Early in the growing season, high resolution yield prediction can support smart farming by providing guidance to farmers on improved targeting of the application of irrigation, pesticides and fertilizers. This also has indirect environmental benefits. Late in the growing season beyond the point at which interventions can be useful, absolute yield prediction and prediction of spatial patterns of yield within fields can be of significant benefit to farms in planning harvest operations and logistics.

Overall crop yield prediction remains a difficult problem, particularly at high spatial resolution and especially early in the growing season. In this work, we have focused principally on the late-stage high-resolution yield prediction problem, with a view to improving harvest planning and logistics. This application is one for which remote sensing has a good chance of making a significant contribution as the technology of high resolution sensing improves in various parts of the electromagnetic spectrum. Also, improvement in this type of yield prediction could generate immediate financial benefits to the farmers concerned.

In this work we have explored the use of both visible/infrared multispectral imagery and multi-polarization synthetic aperture radar imagery at high resolution for late stage high precision summer wheat yield prediction in Europe. The combination of visible, infrared and radar imagery has often been demonstrated to yield superior results in terrestrial remote sensing applications than use of one type of data alone<sup>4</sup>. Our aim has been to predict the spatial pattern of yield within individual fields to within 10% on a grid of 30x30m when compared to the yield as measured by actual combine harvesters as they cut the crop at harvest time. The common use of combine harvesters with GPS positioning and real time yield monitors now makes it possible to obtain spatial patterns of yield within fields and to make comparisons of predicted yield (from remote sensing) with reality.

## 2. EXPERIMENTAL AREA AND DATASETS

### 2.1 Experimental Area

The experimental test area used in this work is in Lincolnshire in the United Kingdom, which is one of the country's foremost agricultural production areas. Lincolnshire is mostly a relatively flat county of the UK which makes it suitable for the use of both visible/infrared and radar imagery without significant terrain distortion effects. The experiments have been carried out on a farm at Riseholme (geographical coordinates: 53 degrees, 15' 54" N; 0 degrees, 32' 36" W; UK Grid reference: SK 984 759 GB). The test fields were planted with wheat. Figure 1 below gives a view of the general test area.



Fig. 1. View of the Riseholme test area (false coloured ASTER image). Image provided by courtesy of NASA.

### 2.2 Satellite data acquired

One of the key aims of this work was to explore the potential for accurate yield prediction using a combination of state of the art operational optical/infrared and radar sensing systems. We chose Terra-1 ASTER imagery for the former because of the number of bands and resolution provided and Envisat ASAR imagery for the latter, with the aim of exploiting not only the use of multi-date radar imagery but also multiple polarization. We obtained multi-temporal images from the ASTER sensor on Terra-1 on the following dates: 10 June 2003, 14 July 2003, 6 August 2003. Envisat ASAR single polarization images were obtained on 24 February 2003, 12 March 2003, 5 May 2003 and 28 June 2003. Dual polarization ASAR images were acquired from Envisat on 2 July 2005 and 6 August 2005. These were in the co-polarization sub-mode, i.e. one HH and one VV image. We requested ASTER images for the 2005 growing season but none were acquired owing to the problem of frequent cloud cover, a problem which has been noted in the past as a significant issue for agricultural remote sensing in Europe<sup>5</sup>.

The ASTER images contain 3 bands in the visible/near infrared (VNIR) at 15m ground resolution, 6 bands in the shortwave infrared (SWIR) at 30m resolution and a further 5 bands in the thermal infrared (TIR) at 90m resolution<sup>6</sup>. For the purposes of this work only the VNIR and SWIR bands were used, i.e. 9 bands in total sampled to a common grid size of 30x30m. The ASAR images have a nominal resolution of 30m<sup>7</sup>. We chose to use radar imagery because of the significant body of evidence of radar sensitivity to crop properties<sup>8,9</sup> and particularly wheat<sup>10,11</sup>, together with evidence of the value of multi-temporal radar<sup>12</sup> and multi-polarization radar imagery<sup>13-17</sup> currently available operationally solely from the ASAR instrument. The ASAR images were all speckle filtered using the adaptive enhanced Lee filter approach<sup>18</sup>.

### 2.3 Ground data from combine harvesters

Ground truth data for the experiments was obtained in the form of digital yield maps obtained by combine harvesters. The maps are created by combining the spot real-time yield measurements made by the harvester as the crop is cut in terms of tons per hectare. The harvester uses a GPS system to locate each spot measurement. An example of a raster image of a yield map for one of the test fields is shown in Figure 2 below. This was obtained by converting 10691 spot

yield samples to a grid and interpolating the data. All the satellite data and ground data were integrated by co-registering and sampling to a common grid using the ENVI image processing package.

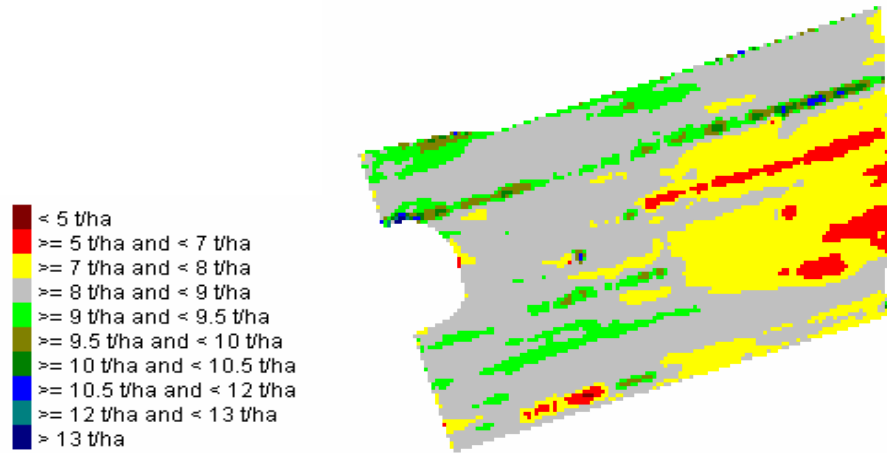


Fig. 2. Wheat yield map obtained from a GPS-enabled combine harvester in the August 2003 harvest. The upper field length is approximately 1km. The field had been planted with winter wheat variety “Tanker”. The field is known as the *Yard 90 Acre* field at the Riseholme Park Farm. There is some evidence of striping in the yield pattern. Although this was initially suspected to be an artifact of the combine harvester sensing system, subsequent investigation found a similar pattern when the field was planted with a pea crop which was harvested by a different machine. This suggests the stripes are a real phenomenon which may be related to the way in which fertilizers or pesticides have been applied in the past.

### 3. YIELD PREDICTION EXPERIMENTS

A variety of yield prediction experiments were carried out using the 2003 and 2005 satellite data. The basic methodology adopted was to use artificial neural networks as the predictors on a pixel by pixel basis, with the satellite image data as input variables. Neural networks were chosen because they have proven particularly effective in integrating multiple types of spatial data in the past<sup>19</sup>, including in agricultural applications<sup>20-23</sup>, and because they can easily be adapted to handle a large number of input variables, as required in a multi-temporal context and with large numbers of channels<sup>24</sup> (for example with hyperspectral imagery<sup>25</sup>) or with combinations of multispectral imagery and multi-polarization imagery as required in this particular application.

#### 3.1 Neural network architectures

We chose to use multilayer perceptron neural networks<sup>26</sup> for as the yield predictors. The basic network architecture used in most of the experiments was a N-10-10-1 architecture, i.e. N satellite variables as inputs, a first hidden layer with 10 neurons, a second hidden layer with 10 neurons and a single output layer node whose value should represent the yield for the pixel in question. The networks were trained with 10% of the actual yield sample in most of the experiments. The network was trained to learn the relationships between the input satellite variables and the actual combine harvester measurements of the crop yield. All of the satellite data and the ground data were geographically co-referenced as a stack of spatial data layers. The architecture of the neural networks is shown in Figure 3.

The neural networks were implemented using a state-of-the-art package known as Trajan<sup>27</sup>. The training procedure used the quasi-Newton approach for error minimization. Testing of network performance was obtained with a further 10% of the available yield samples, which were spatially uncorrelated with the training data.

#### 3.2 Yield prediction using multi-temporal ASTER imagery

The first set of experiments was concerned with late season yield prediction using only multi-temporal ASTER data. The three images from June, July and August 2003 were used each with the 9 spectral bands (VNIR +SWIR). In addition, a normalized difference vegetation index (NDVI) image was computed and used as a tenth band for each image, thus giving a total of 30 individual satellite-derived input variables for yield prediction (i.e. N=30 in this case).

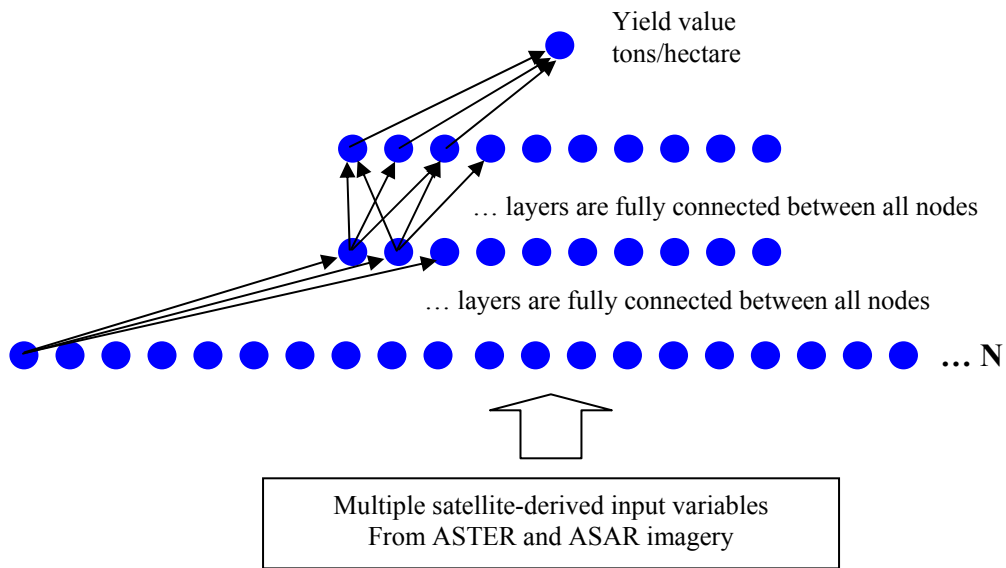


Fig. 3. Neural network architecture adopted for the single network experiments. The basic architecture consisted of a multilayer perceptron with 2 hidden layers each containing 10 nodes. Training was performed with the quasi-Newton method.

For the multi-temporal ASTER image experiment with 30 inputs, a total of 1069 training samples were used and the training ran for 451 epochs, until no appreciable change in error level occurred. The trained neural network was then used to generate a predicted yield map covering an entire field. The resulting predicted yield map is shown in Figure 4 below.

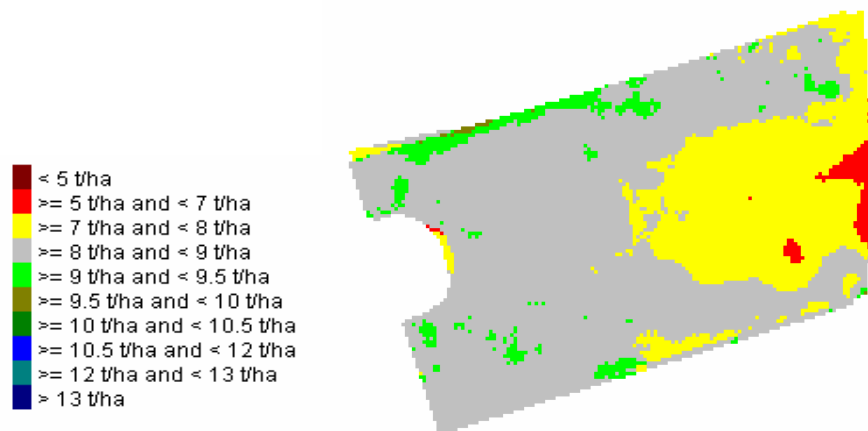


Fig. 4. Predicted wheat yield map obtained from late season three-date Terra ASTER imagery. Yard 90 Acre field at Riseholme Park Farm, Lincolnshire, UK. Prediction obtained from 30-10-10-1 multilayer perceptron neural network.

Visually the predicted yield map matches reasonably well to the actual yield map derived from the combine harvester (as shown in Figure 2), although there are some clear differences. For example the overall pattern of reduced yield on the right hand side and enhanced yield towards the top of the field is clearly predicted, however the narrow strips of actual elevated yield are not predicted from the satellite data. The results are assessed quantitatively in section 4 below.

### 3.3 Yield prediction using ENVISAT ASAR imagery

The second experiment was carried out to establish the potential of multi-temporal ASAR data alone to predict wheat yield. ASAR data has the advantage over ASTER imagery of being more readily available at high latitudes since it is not significantly affected by cloud cover. This is an important advantage in many European countries where wheat production is an important part of the agricultural economy. High yield requires adequate rainfall which implies more cloudiness on average, thus interfering with crop monitoring at visible and infrared wavelengths.

In this experiment the four single polarization ASAR images from February, March, May and June 2003 were used (i.e. N=4). The training set again consisted of 1069 samples, though the training was run for somewhat longer through a total of 1289 epochs. In this case, the much lower dimensionality of the input data resulted in a slower convergence to an acceptable error level. The predicted yield map is shown in Figure 5.

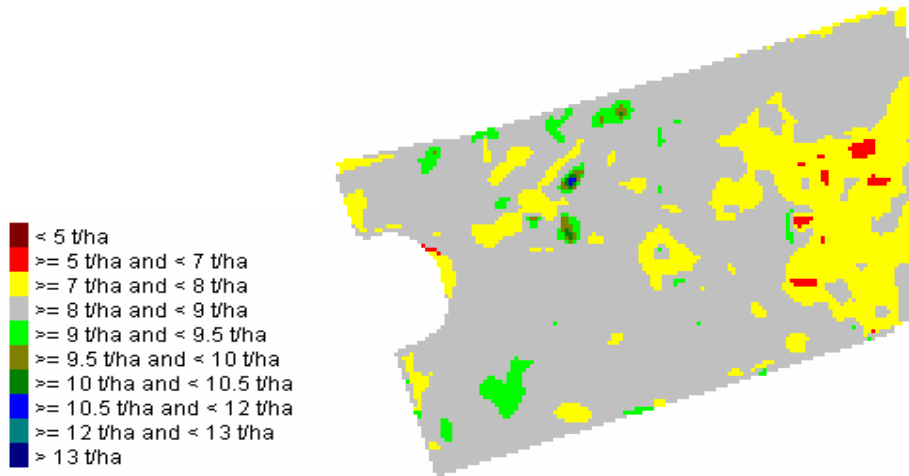


Fig. 5. Predicted wheat yield map obtained from four-date Envisat ASAR imagery. Yard 90 Acre field at Riseholme Park Farm, Lincolnshire, UK. Prediction obtained from 4-10-10-1 multilayer perceptron neural network.

The result in Figure 5 shows that the ASAR imagery alone is able to predict the broad pattern of actual yield (i.e. compare with Figure 2). The reduced yield area to the right of the field is correctly picked out in the ASAR data. However other detail has been lost and the overall result is not as good as that obtained from the multi-temporal ASTER imagery. Nevertheless there is an implication from the result that multi-temporal synthetic aperture radar data is capable of providing some useful information about potential wheat yield.

### 3.4 Yield prediction using integrated ASTER imagery, NDVI and multi-temporal ASAR imagery

For the third experiment, we chose to integrate the multi-temporal ASTER and multi-temporal ASAR imagery including use of the computed NDVI band. In total this provided an integrated satellite data set comprising 34 separate channels or neural network input variables, i.e. 3 dates of 9 channel ASTER images plus 3 dates of NDVI combined with 4 dates of single polarization ASAR imagery.

The result from the combined sensor approach is shown in Figure 6. Interestingly the overall pattern of yield is predicted more faithfully than by the use of the ASAR data alone, though the pattern is not significantly improved in comparison to the ASTER data alone (Figure 4). However, the combined data set does more correctly predict the area of low yield in the bottom left part of the scene, where indicated on the figure. It is not clear why the combination of sensors has improved the prediction of the yield pattern in this part of the field, particularly as the reduced yield is not evident in this area in either of the separate ASTER-only or ASAR-only predictions.

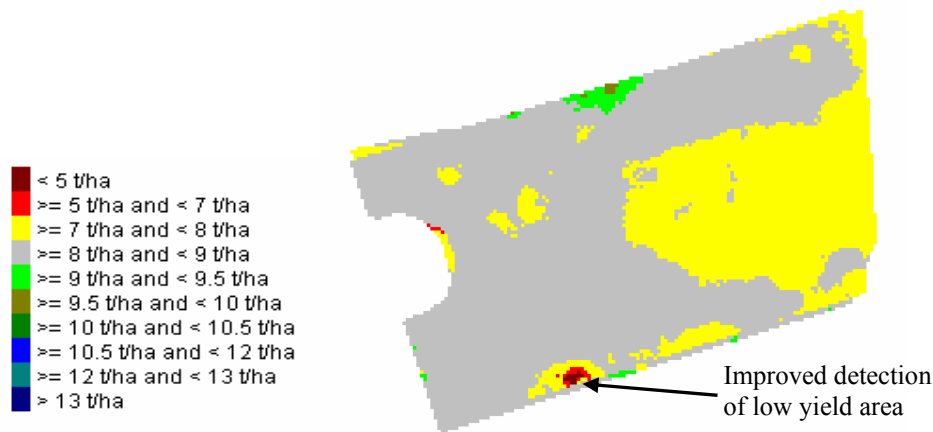


Fig. 6. Predicted wheat yield map obtained from combined three-date ASTER imagery, NDVI data and four-date Envisat ASAR single polarization imagery (34 input variables). Yard 90 Acre field at Riseholme Park Farm, Lincolnshire, UK. Prediction obtained from 34-10-10-1 multilayer perceptron neural network.

### 3.5 Use of neural network ensembles

It is well known that separate randomly initialized neural networks may converge to different solutions to the same overall pattern recognition or prediction problem. This has led to a number of neural network applications based on competing or voting ensembles of networks in which a deliberate attempt is made to harness the increased potential of multiple solutions to the same problem. Such ensemble networks are considered to help combat over-fitting problems and improve overall generalization.

An experiment was conducted using the separate networks trained with the ASTER data and the ASAR data respectively but combined as though they were separate members of an ensemble of networks trained to solve the same prediction problem. For each separate spatial location in the field, the outputs from the two networks described in sections 3.2 and 3.3 were combined to derive a single yield prediction. This was done by producing a single weighted sum. The weighting was based on the relative correlation factors between the predicted and actual yields as revealed in testing the individual networks. In this case the ASTER network was weighted at 0.7 and the ASAR network at 0.5. The result of this process is shown in Figure 7.

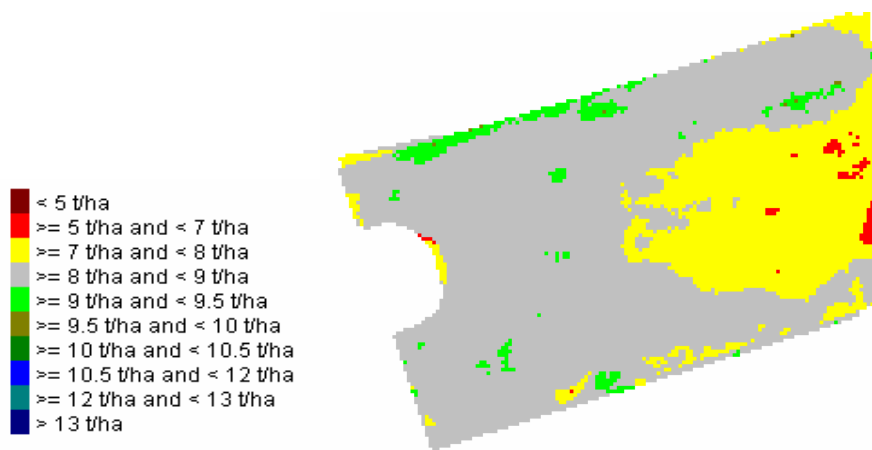


Fig. 7. Predicted wheat yield map obtained from combined three-date ASTER imagery, NDVI data and four-date Envisat ASAR single polarization imagery. Yard 90 Acre field at Riseholme Park Farm, Lincolnshire, UK. Prediction obtained from weighted ensemble of 30-10-10-1 (weighting factor 0.7) and 4-10-10-1 (weighting factor 0.5) multilayer perceptron neural networks.

### 3.6 Inter-field generalization of neural network yield predictor

One of the key issues in the use of neural networks is the extent to which they can generalize and generate acceptable results in new situations. In this case, it is highly desirable that a neural network trained to predict crop yield in one locality can also accurately predict yield of the same crop in a different locality. In order to evaluate the generalization capability of the neural networks we conducted an experiment to determine how a neural network trained on one field would perform in predicting wheat yield in another using the same data sources, i.e. ASTER plus ASAR data. In this experiment, a network was trained with data from the *Yard 90 Acre Field* to predict yield from 3-date ASTER imagery + NDVI + 4-date ASAR imagery as described in section 3.4. The neural network had 34 inputs and 10 nodes in each hidden layer as in the previous experiments. This neural network was then “ported” to a different context –i.e. used to predict yield in a different field (known as “*Ben’s field*”) at Riseholme using the same image data sets. Figure 8 shows the actual yield as measured by the combine harvester in August 2003 and Figure 9 shows the neural network prediction of yield based on the use of the ASTER and ASAR images.

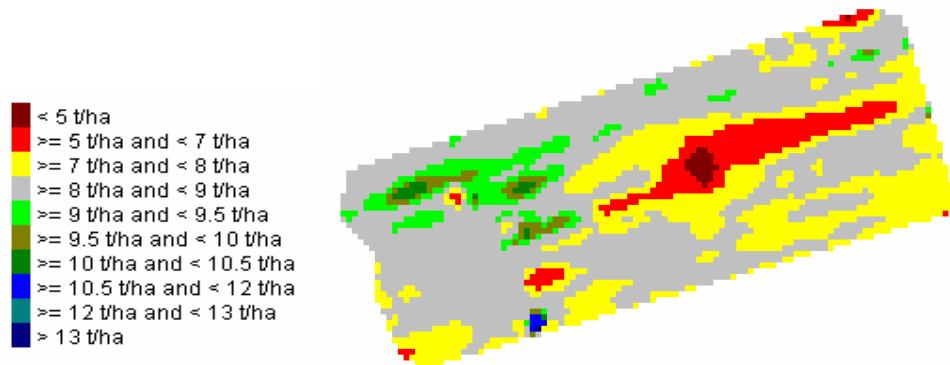


Fig. 8. Actual wheat yield map obtained from a GPS-enabled combine harvester in the August 2003 harvest for “*Ben’s Field*” at the Riseholme Park Farm. (Wheat variety: “*Tanker*”).



Fig. 9. Generalization test showing predicted wheat yield map obtained from combined three-date ASTER imagery, NDVI data and four-date Envisat ASAR single polarization imagery. “*Ben’s field*” at Riseholme Park Farm, Lincolnshire, UK. Prediction obtained from a 34-10-10-1 multilayer perceptron neural network trained with data from “*Yard 90 Acre*” field (1069 training samples, equivalent to 10% of available training data, randomly selected).

Visually it can be seen that the neural network has correctly predicted the broad area of reduced yield in the centre right of the field (Figure 9.). However the area is much more compact than in the actual yield map (Figure 8.). A quantitative evaluation of the prediction performance follows in section 4.

### 3.7 Yield prediction using multi-temporal dual polarization images

In addition to the experiments on yield prediction using ASTER imagery plus single polarization ASAR images, we wished also to test the use of multi-temporal multi-polarization radar images for yield prediction. Requests were made to the European Space Agency for a series of dual polarization (VV&HH) ASAR images to be acquired during the summer

of 2005. However, owing to operational constraints and conflicting user requests, only two such images were acquired for our test area as described in section 2 on 2 July 2005 and 6 August 2005, shortly before the harvest. As in the earlier experiments, ground truth yield data was obtained from the GPS-enabled combine harvester which took real-time yield measurements during the 2005 harvest (Figure 10).

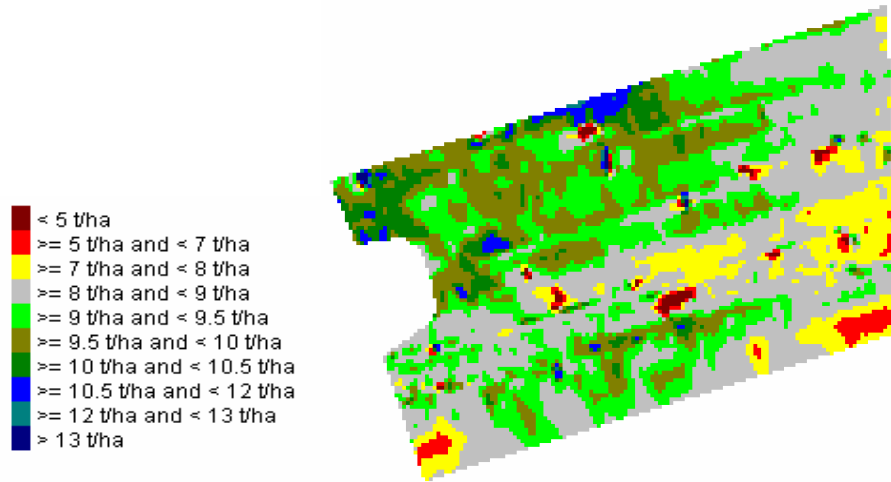


Fig. 10. Wheat yield map obtained from a GPS-enabled combine harvester in the August 2005 harvest. The field had been planted with wheat variety “Einstein”. (Yard 90 Acre field at the Riseholme Park Farm).

A multilayer perceptron neural network was trained to predict the wheat yield using the four channels of radar data as its input (i.e. a 4-10-10-1 architecture). These four inputs were the HH backscatter signal for 2 July, the VV backscatter signal for 2 July, the HH backscatter signal for 6 August and the VV backscatter signal for 6 August. The neural network was trained with 10% of the available samples (1130 training samples used) using the backpropagation algorithm. The results of the yield prediction are shown in Figure 11.

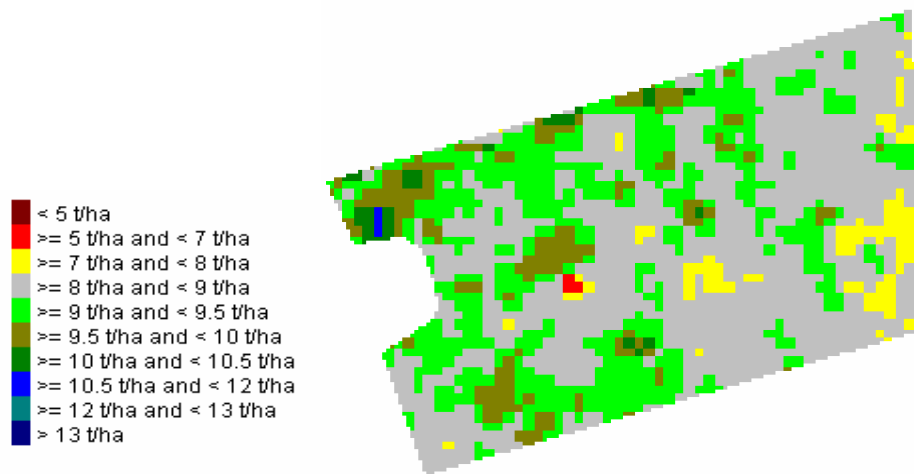


Fig. 11. Predicted wheat yield map obtained from multi-polarization Envisat ASAR imagery. Yard 90 Acre field at Riseholme Park Farm, Lincolnshire, UK. Prediction obtained from 4-10-10-1 multilayer perceptron neural network with four input channels (two dates of HH & VV polarization in 2005).

It is interesting to note that in broad terms, there is some degree of commonality between the actual yield map and the predicted yield map based on the 2-date multi-polarization ASAR imagery. However at the detailed pixel level there are significant differences.

We also investigated whether the capability of the multi-polarization data to predict yield could be enhanced by use of ancillary information. Ideally ASTER data should have been used for this, but none was available for the latter part of the 2005 growing season owing to cloud cover. Instead we investigated whether or not yield data from a previous year could influence the accuracy of yield prediction. Although this might seem unexpected, there is some reason to believe that yield patterns may be subject to a “memory effect” –i.e. with yields partly mirroring yields from previous years possibly as a result of localized soil conditions or previous patterns of heavy fertilizer application retained by the soil. In order to test this, we trained a neural network with the four channels of ASAR data from 2005 plus the actual yield data from 2003 as a separate channel (i.e. a 5-10-10-1 network architecture). The result from this is shown in Figure 12. Overall there is a small improvement in the quality of the yield prediction.

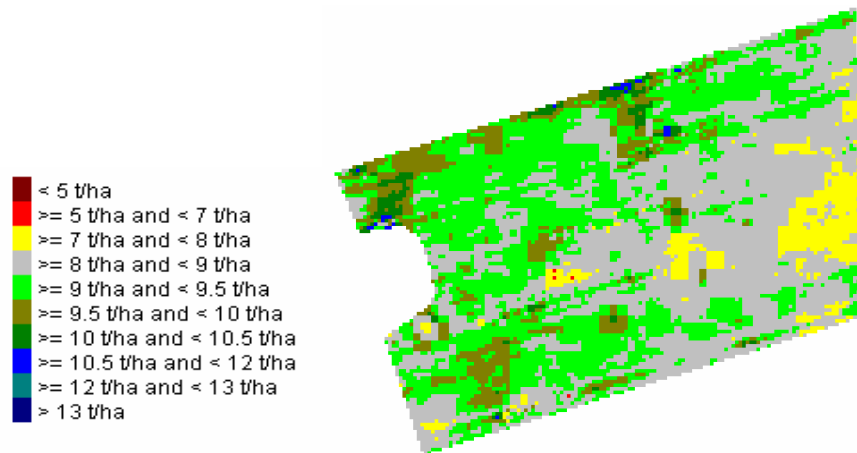


Fig. 12. Field “memory effect” test. Predicted wheat yield map obtained from multi-polarization Envisat ASAR imagery. Yard 90 Acre field at Riseholme Park Farm, Lincolnshire, UK. Prediction obtained from 5-10-10-1 multilayer perceptron neural network with five input channels (two dates of HH & VV polarization in 2005 plus 2003 yield).

### 3.8 Use of neural network ensemble with multi-temporal dual polarization radar

We also investigated the use of an ensemble of neural networks to predict yield based on the multi-temporal dual polarization radar data. We used two networks trained separately as follows: (i) Network 1: the 2 July 2005 HH and VV images plus 2003 yield, (ii) Network 2: the 6 August 2005 HH and VV images plus 2003 yield. Both networks had a 3-10-10-1 architecture. The result is shown in Figure 13.

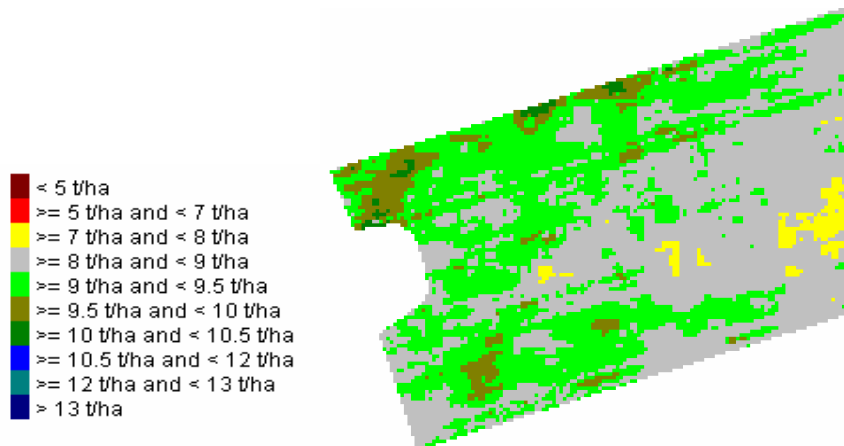


Fig. 13. Predicted wheat yield map obtained from multi-polarization Envisat ASAR imagery, August 2005. Prediction obtained from two 3-10-10-1 multilayer perceptron neural networks with equal weighting.

## 4. QUANTITATIVE EVALUATION OF THE RESULTS

### 4.1 Discussion of the results

The quantitative results for all of the experiments conducted are shown in Table 1. A number of interesting observations can be made from these results as follows, based mainly on the overall correlation figures (bottom row) between the actual yield and predicted yields:

- (i) It is clear that multi-temporal VNIR data from ASTER is more effective for yield prediction than multi-temporal single polarization ASAR imagery.
- (ii) A combination of 3-date ASTER imagery and 4-date ASAR imagery can predict yield maps with an overall correlation of 0.71. This rises to 0.77 when a multiple neural network predictor is used.
- (iii) The neural network predictors do not “port” effectively between different localities which is a significant constraint in developing operational yield prediction systems (correlation only 0.42).
- (iv) Multi-temporal multi-polarization ASAR data is not by itself sufficient to generate a good yield prediction (correlation 0.45), though the accuracy can be improved by exploiting an apparent field memory effect and by using a neural network ensemble –though still not to acceptable levels (correlation 0.52 and 0.56 respectively).

Table. 1. Quantitative results for each yield prediction experiment. The bottom row indicates the overall correlation between the predicted yield from the satellite data+neural network and the actual yield measured by the combine harvester.

Quantitative Experimental Results								
	3-date ASTER +NDVI	4-date ASAR (single pol.)	ASTER +NDVI +ASAR	ASTER +NDVI +ASAR: NN ensemble	General- ization: NN ported	2-date VV&HH ASAR	2-date VV&HH ASAR +2003 yield	2-date VV&HH ASAR +2003 yield: NN ensemble
<b>Data mean</b>	8.2538	8.2538	8.2538	8.2538	8.105	8.9234	8.9234	8.9234
<b>Data S.D.</b>	0.80587	0.80587	0.80587	0.80587	0.97013	0.98039	0.98039	0.98039
<b>Error mean</b>	-0.01854	0.037258	0.025993	0.009353	0.13061	-0.01699	-0.00236	-0.00049
<b>Error S.D.</b>	0.56539	0.6894	0.56922	0.52395	0.96179	0.87862	0.83876	0.82396
<b>Abs. Error mean</b>	0.36222	0.48671	0.39813	0.32957	0.66015	0.58875	0.55083	0.53053
<b>S.D. ratio</b>	0.70159	0.85548	0.70634	0.65017	0.9914	0.89619	0.85553	0.84043
<b>Correlation</b>	<b>0.71274</b>	<b>0.52281</b>	<b>0.71395</b>	<b>0.77021</b>	<b>0.4214</b>	<b>0.4473</b>	<b>0.51973</b>	<b>0.55579</b>

## 5. CONCLUSIONS

In this work we have investigated the capability of combinations of multi-temporal visible/near-infrared imagery and multi-temporal synthetic aperture radar imagery to predict within-field patterns of wheat yield using artificial neural network predictors. In principle the use of 9-channel (VNIR+SWIR) ASTER imagery plus dual polarization ASAR data offers a very powerful operational tool for land resource remote sensing at high spatial resolution especially when used multi-temporally. The results from the experiments demonstrate that combinations of such different types of data can improve yield prediction performance, though there is some way to go to get to the original target of less than 10% error. The range of the experiments reported in this paper has been limited so far by operational constraints on acquiring satellite data (heavy user demands on the Envisat ASAR sensor, and cloud cover interfering with ASTER image

acquisitions). This has so far prevented a test of the full capability of multi-temporal multi-polarization radar image sequences along with sequences of multi-temporal multi-channel VNIR+SWIR data imagery and there is still scope for further work if good multi-temporal datasets can be obtained from both sensors in the same season.

It is also interesting to note from this work that yield prediction accuracy can be influenced by the choice of predictive algorithm, e.g. based on ensembles of artificial neural networks rather than single networks. However evidence from other work in remote sensing has shown that a range of computational intelligence approaches can be used in geophysical parameter estimation and we therefore believe there is scope for more experimentation in this area also. This could include, for example, supplementing the neural network approaches with evidential reasoning methods that could more effectively make use of background knowledge and possible field memory effects as part of the overall predictive system.

Overall as both remote sensing technologies improve, and the analysis algorithms become more sophisticated, we can expect further improvements in the potential for operational prediction of actual cereal crop yields late in the growing season. This is a very real challenge in remote sensing, but one that is potentially achievable operationally.

## 6. ACKNOWLEDGMENTS

The authors are grateful to the European Space Agency for provision of Envisat ASAR data within the Category-1 project C1P-3141 entitled: "Application of Fused ASAR dual polarization data and high resolution visible-infrared data to cereal yield prediction in smart farming" and also to NASA JPL for authorized user access to ASTER data sets. The authors are also extremely grateful to Mr. Jeremy Nicholson of Leverton Farms and to Mr. Clive Bound and staff of the Lincolnshire School of Agriculture, for access to the farm and provision of combine harvester yield data.

## 7. REFERENCES

1. P. J. Pinter, J. L. Hatfield, J. S. Schepers, E. M. Barnes, M. S. Moran, C. S. T. Daughtry and D. R. Upchurch, "Remote sensing for crop management", *Photogrammetric Engineering and Remote Sensing* 69(6), 647-664 (2003).
2. P. C. Doraiswamy, S. Moulin, P. W. Cook and A. Stern, "Crop yield assessment from remote sensing", *Photogrammetric Engineering and Remote Sensing* 69(6), 665-674 (2003).
3. R. A. Roebeling, E. Van Putten, G. Genovese and A. Rosema, "Application of Meteosat derived meteorological information for crop yield predications in Europe", *Int. J. Remote Sensing* 25(23), 5389-5401 (2004).
4. J. Li and W. Chen, "A rule-based method for mapping Canada's wetlands using optical, radar and DEM data", *Int. J. Remote Sensing* 26(22), 5051-5069 (2005).
5. C. Kontoes and J. Stakenborg, "Availability of cloud-free Landsat images for operational projects. The analysis of cloud-cover figures over the countries of the European Community", *Int. J. Remote Sensing* 11(9), 1599-1608 (1990).
6. ASTER sensor information: <http://edcdaac.usgs.gov/aster/asteroverview.asp>
7. Envisat ASAR image product details: <http://envisat.esa.int/dataproducts/asar/CNTR.htm>
8. G. Macelloni, S. Paloscia, P. Pampaloni, F. Marliani and M. Gai, "The relationship between the backscattering coefficient and the biomass of narrow and broad leaf crops", *IEEE Trans. Geoscience and Remote Sensing* 39(4), 873-884 (2001).
9. A. Della Vecchia, P. Ferrazzoli, L. Guerriero, X. Blaes, P. Defourny, L. Dente, F. Mattia, G. Satalino, T. Strozzi and U. Wegmüller, "Influence of geometrical factors on crop backscattering at C-Band", *IEEE Trans. Geoscience and Remote Sensing* 44(4), 778-790 (2006).
10. S. M. Brown, S. Quegan, K. Morrison, J. C. Bennett and G. Cookmartin, "High-resolution measurements of scattering in wheat canopies –implications for crop parameter retrieval", *IEEE Trans. Geoscience and Remote Sensing* 41(7), 1602-1610 (2003).
11. D. Singh, Y. Yamaguchi and H. Yamada, "Retrieval of wheat chlorophyll by an X-band scatterometer", *Int. J. Remote Sensing* 24(23), 4939-4951 (2003).
12. B. Tso and P. M. Mather, "Crop discrimination using multi-temporal SAR imagery", *Int. J. Remote Sensing* 20(12), 2443-2460 (1999).
13. G. M. Foody, M. B. McCulloch and W. B. Yates, 1994. "Crop classification from C-band polarimetric radar data", *Int. J. Remote Sensing* 15(14), 2871-2885 (1994).
14. J. L. Gómez-Dans, S. Quegan and J. C. Bennett, "Indoor C-Band polarimetric interferometry observations of a mature wheat canopy", *IEEE Trans. Geoscience and Remote Sensing* 44(4), 768-777 (2006).

15. J.-S. Lee, M. R. Grunes and E. Pottier, "Quantitative comparison of classification capability: fully polarimetric versus dual and single-polarization SAR, *IEEE Trans. Geoscience and Remote Sensing* 39(11), 2343-2351 (2001).
16. J. D. Ballester-Berman, J. M., Lopez-Sanchez and J. Fortuny-Guasch, "Retrieval of biophysical parameters of agricultural crops using polarimetric SAR interferometry", *IEEE Trans. Geoscience and Remote Sensing* 43(4), 683-694 (2005).
17. K. A. Stankiewicz, "The efficiency of crop recognition on ENVISAT ASAR images in two growing seasons", *IEEE Trans. Geoscience and Remote Sensing* 44(4), 806-814 (2006).
18. A. Lopes, R. Touzi and E. Nezry, "Adaptive speckle filters and scene heterogeneity", *IEEE Trans. Geoscience and Remote Sensing* 28(6), 992-1000 (1990).
19. H. Mills, M. E. J. Cutler, and D. Fairbairn, "Artificial neural networks for mapping regional-scale upland vegetation from high spatial resolution imagery", *Int. J. Remote Sensing* 27(11), 2177-2195 (2006).
20. C. Chen and H. McNairn, "A neural network integrated approach for rice crop monitoring", *Int. J. Remote Sensing* 27(7-8), 1367-1393 (2006).
21. D. Jiang, X. Yang, N. Clinton and N. Wang, "An artificial neural network for estimating crop yields using remotely sensed information, *Int. J. Remote Sensing* 25(9), 1723-1732 (2004).
22. C. S. Murthy, P. V. Raju and K. V. S. Badrinath, "Classification of wheat crop with multi-temporal images: performance of maximum likelihood and artificial neural networks, *Int. J. Remote Sensing* 24(23), 4871-4890 (2003).
23. F. M. Danson, C. S. Rowland and F. Baret, "Training a neural network with a canopy reflectance model to estimate crop leaf area index", *Int. J. Remote Sensing* 24(23), 4891-4905 (2003).
24. I. Kanellopoulos, A. Varfis, G. G. Wilkinson and J. M egier, "Land cover discrimination in SPOT imagery by artificial neural network -a twenty class experiment", *Int. J. Remote Sensing* 13(5), 917-924 (1992).
25. L. Estep, G. Terrie and B. Davis, "Crop stress detection using AVIRIS hyperspectral imagery and artificial neural networks", *Int. J. Remote Sensing* 25(22), 4999-5004 (2004).
26. I. Kanellopoulos and G. G. Wilkinson, "Strategies and best practice for neural network image classification", *Int. J. Remote Sensing* 18(4), 711-725 (1996).
27. Trajan neural network simulator: <http://www.trajan-software.demon.co.uk/>